

Comprehensive study of equilibrium structure of trans-azobenzene: gas electron diffraction and quantum chemical calculations

Alexander E. Pogonin^{1,*}, Ivan Yu. Kurochkin², Alexey V. Eroshin³, Maksim N. Zavalishin⁴ and Yuriy A. Zhabanov ^{2,*}

¹ Department of Ceramics Technology and Electrochemical Production, Ivanovo State University of Chemistry and Technology, Sheremetevskiy av. 7, 153000 Ivanovo, Russia

² Department of Physics, Ivanovo State University of Chemistry and Technology, Sheremetevskiy av. 7, 153000 Ivanovo, Russia; ivan.kurochkin.95@bk.ru (I.Y.K.)

³ Department of Physical and Colloidal Chemistry, Ivanovo State University of Chemistry and Technology, Sheremetevskiy av. 7, 153000 Ivanovo, Russia; alexey.yeroshin@gmail.com

⁴ Department of General Chemical Technology, Ivanovo State University of Chemistry and Technology, Sheremetevskiy av. 7, 153000 Ivanovo, Russia; zavalishin00@gmail.com

* Correspondence: pogonin@isuct.ru, zhabanov@gmail.com

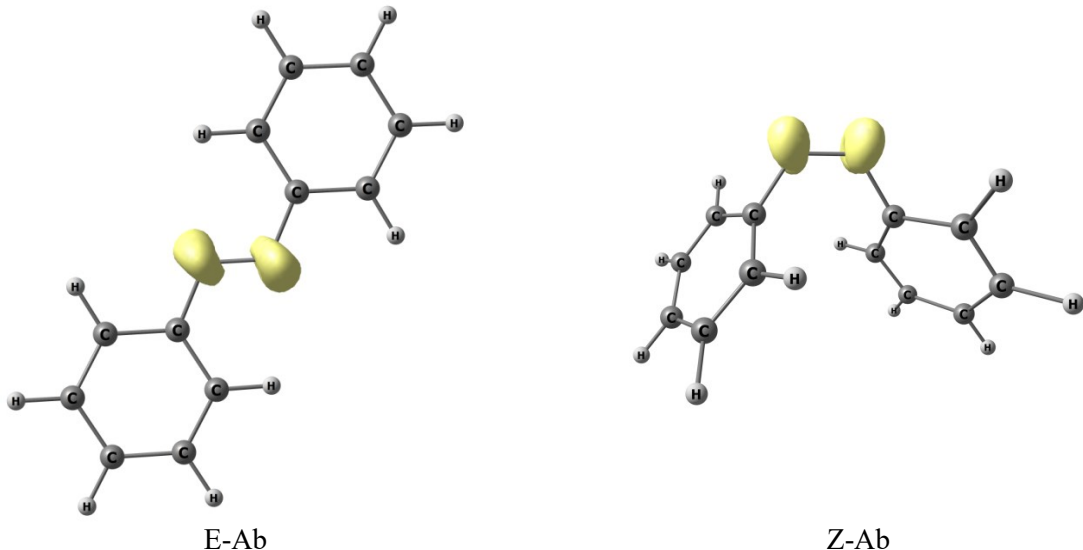


Figure S1. FOD plot for AB. The FOD plots were generated with the “orca-plot” utility program included in the ORCA. A density plot with resolution $120 \times 120 \times 120$ was generated from the FOD after TPSS/def2-TZVP/ $T_{el}=5000\text{K}$ finite temperature SCF iterations in B3LYP/pcseg-2 optimized geometry were converged. Visualization of FOD plot (in yellow) made by the ChemCraft program with Contour value 0.005.

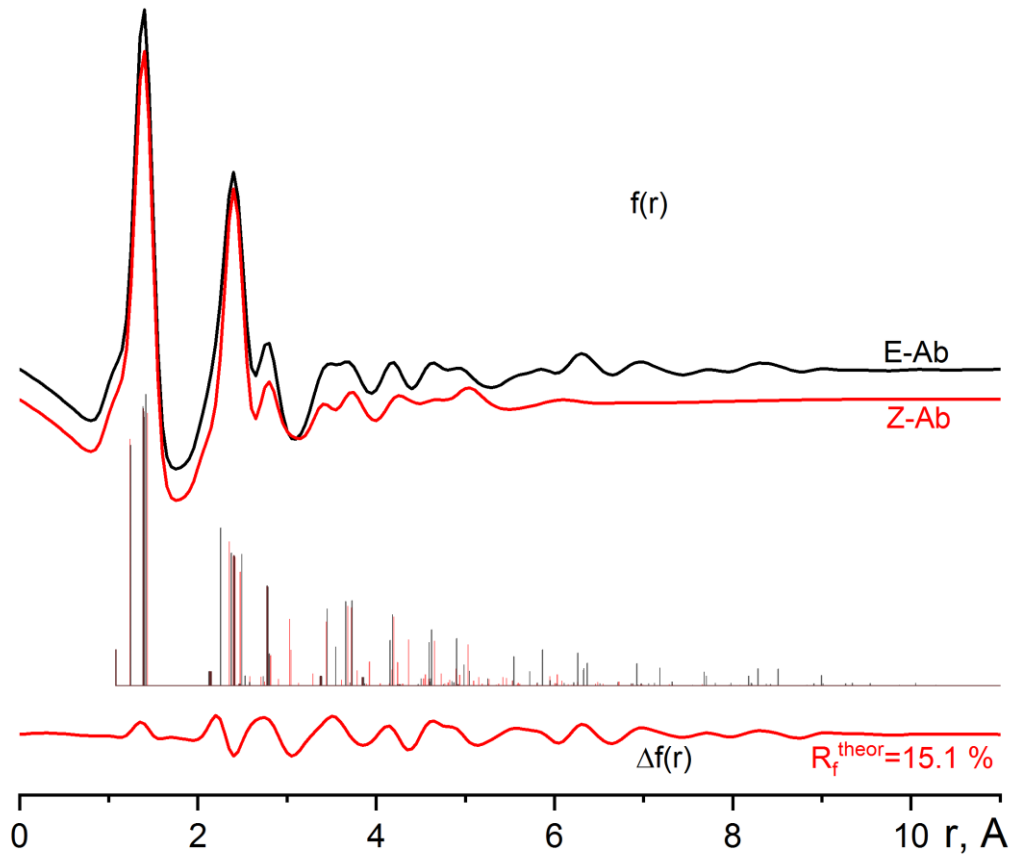


Figure S2. Comparison of theoretical radial distribution functions $f(r)$ of E-AB and Z-AB.

Calculations of the theoretical radial distributions curves $f(r)$ were performed using classic mode in the UNEX program. It is essentially a sine-Fourier transformation of corresponding theoretical molecular scattering intensities $sM(s)$ curves

$$f(r) = \int_{s_{min}}^{s_{max}} sM(s) \sin(sr) e^{-bs^2} ds$$

where $f(r)$ is radial distributions curve, $sM(s)$ – theoretical molecular scattering intensities curve, s – scattering variable, r – internuclear distances, b – damping factor, R_f^{theor} – a factor of disagreement between theoretical molecular scattering intensities $sM(s)$ of Z-AB and planar E-AB which was calculated as:

$$R_f^{theor} = \sqrt{\frac{\sum_{i=1}^N (s_i M(s_i)_{Z-AB} - k_M s_i M(s_i)_{E-AB})^2}{\sum_{i=1}^N (s_i M(s_i)_{Z-AB})^2}} \cdot 100\%$$

where $s_i M(s_i)$ are theoretical molecular scattering intensities; k_M is the scale factor. Differences function $\Delta f(r)$ was calculated concerning planar E-AB – $\Delta f(r) = f_{Z-AB}(r) - f_{E-AB}(r)$. Molecular parameters were calculated at B3LYP-D3/pcseg-2 theory level. Vibrational amplitudes and corrections ($r_{h1}-r_a$) were obtained from the harmonic force fields using the VibModule program for the B3LYP-D3/pcseg-2 calculations.

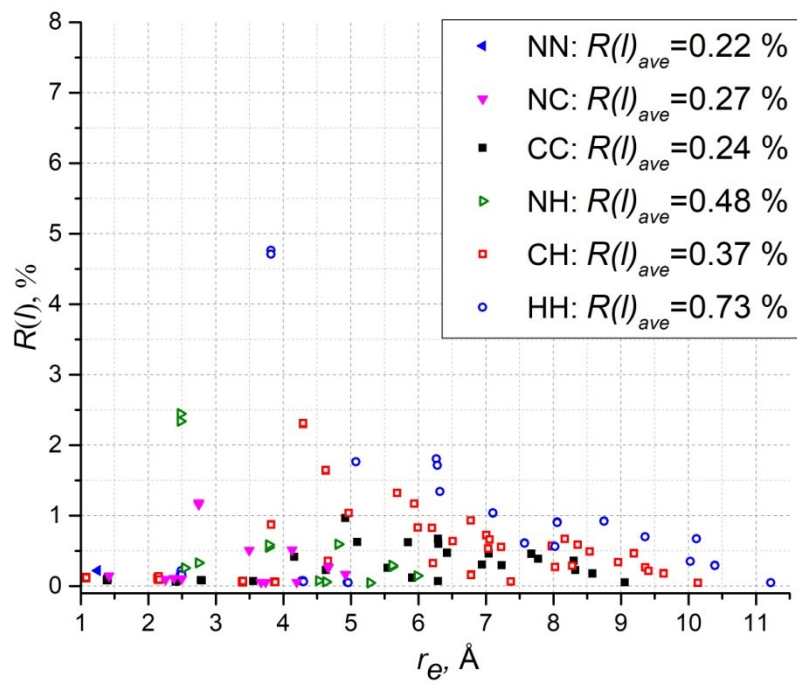


Figure S3. Relative ranges of vibrational amplitudes $R(l)$ for pairs of atoms X_i and Y_j ($X_i, Y_j = H, C, N$) determined by equation (8). To determine vibrational amplitudes l , the results of calculations with 13 different DFT functionals (B3LYP, B97D, B98, BMK, BP86, CAM-B3LYP, M06, mPW1PW91, PBE, PBE0, TPSSh, VSXC, X3LYP) were used.

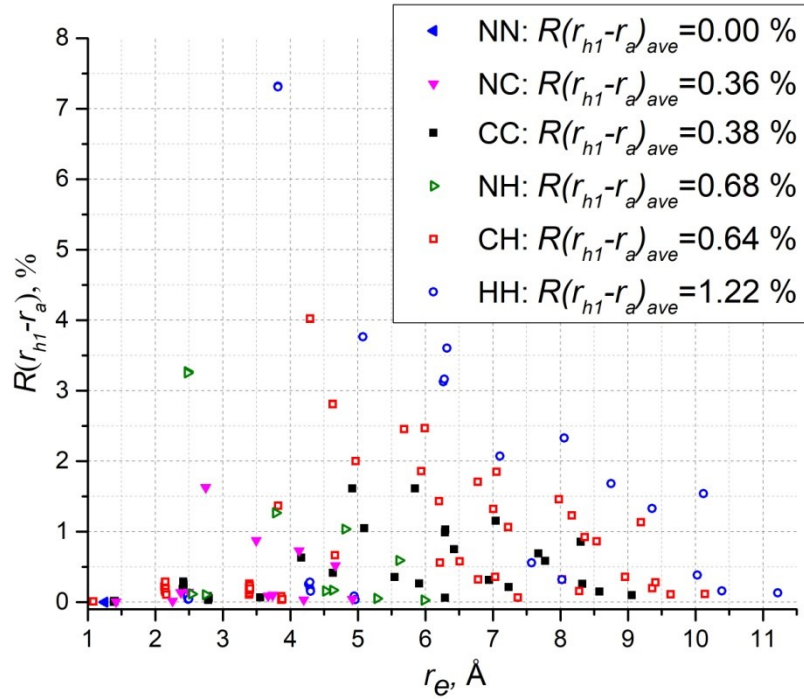


Figure S4. Relative ranges of vibrational corrections $R(r_{h1} - r_a)$ for pairs of atoms X_i and Y_j ($X_i, Y_j = H, C, N$) determined by equation (3). To determine vibrational corrections $r_{h1} - r_a$, the results of calculations with 13 different DFT functionals (B3LYP, B97D, B98, BMK, BP86, CAM-B3LYP, M06, mPW1PW91, PBE, PBE0, TPSSh, VSXC, X3LYP) were used.

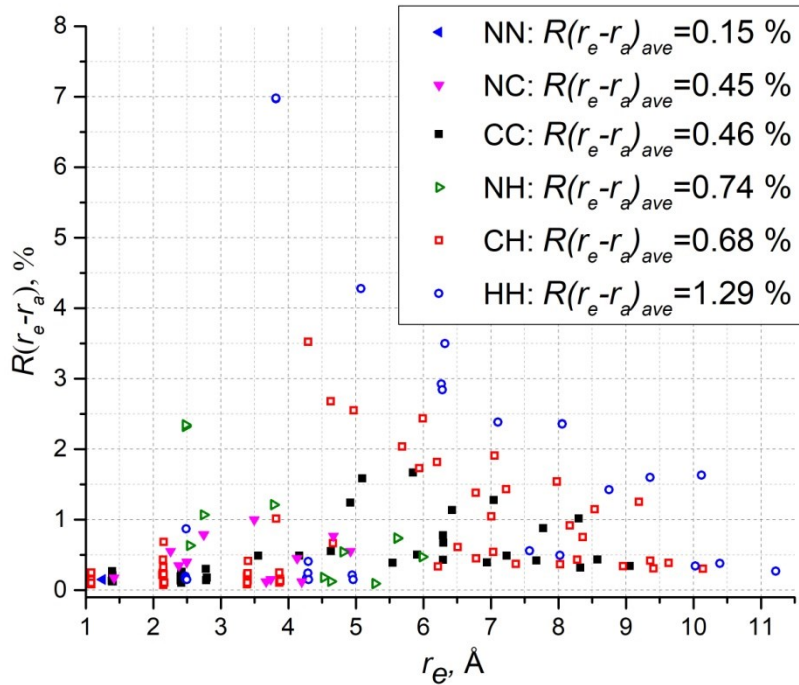


Figure S5. Relative ranges of vibrational corrections $R(r_e - r_a)$ for pairs of atoms X_i and Y_j ($X_i, Y_j = H, C, N$) determined by equation (8). To determine vibrational corrections $r_e - r_a$, the results of calculations with 13 different DFT functionals (B3LYP, B97D, B98, BMK, BP86, CAM-B3LYP, M06, mPW1PW91, PBE, PBE0, TPSSh, VSXC, X3LYP) were used.

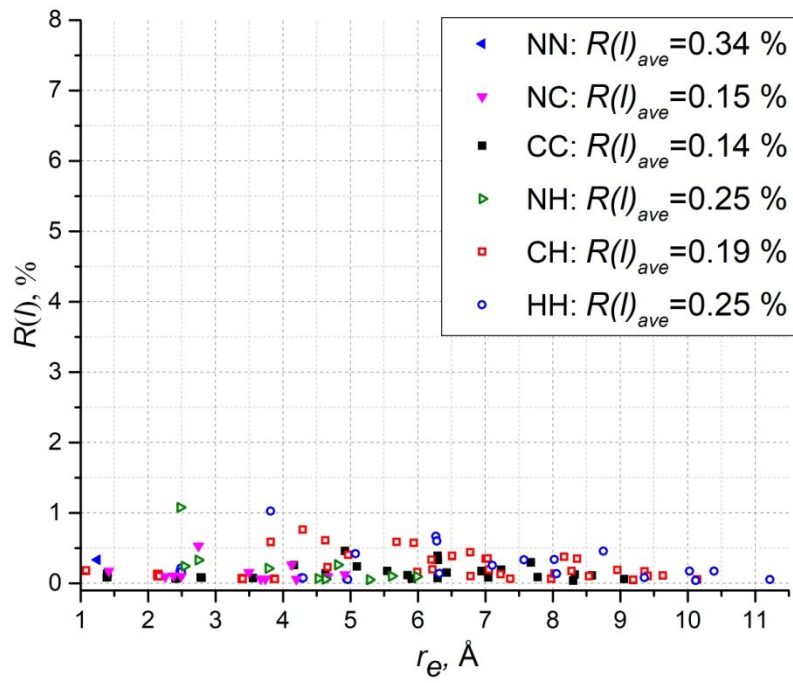


Figure S6. Relative ranges of vibrational amplitudes $R(l)$ for pairs of atoms X_i and Y_j ($X_i, Y_j = H, C, N$) determined by equation (8). To determine vibrational amplitudes l , the results of calculations with 16 different DFT functionals (B3LYP, B97D, B98, BMK, BP86, CAM-B3LYP, LC-wPBE, M05, M06, M06HF, mPW1PW91, PBE, PBE0, TPSSh, VSXC, X3LYP) were used. The first frequency corresponding to phenyl moieties rotations was ignored when calculating the vibrational amplitudes l .

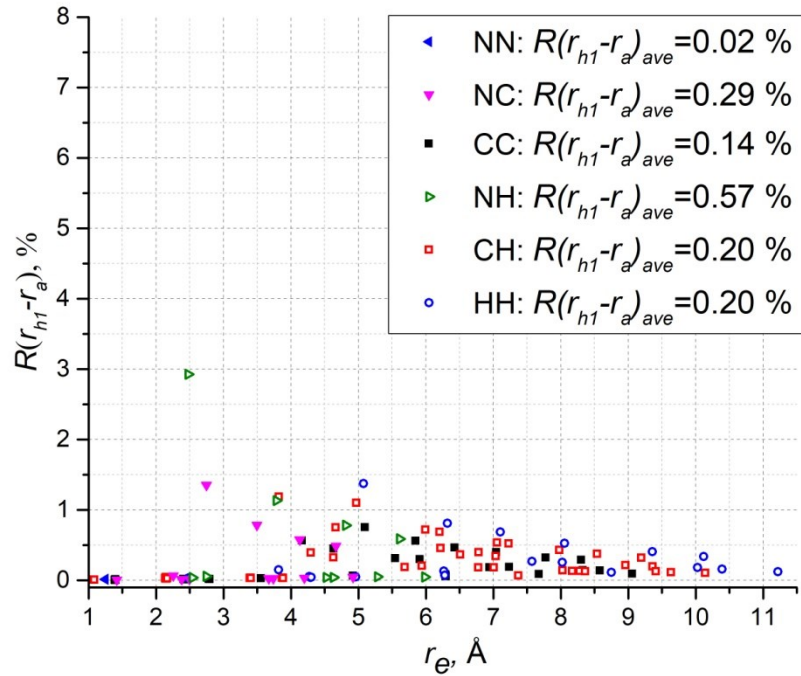


Figure S7. Relative ranges of vibrational corrections $R(r_{h1} - r_a)$ for pairs of atoms X_i and Y_j ($X_i, Y_j = H, C, N$) determined by equation (8). To determine vibrational corrections $r_{h1} - r_a$, the results of calculations with 16 different DFT functionals (B3LYP, B97D, B98, BMK, BP86, CAM-B3LYP, LC-wPBE, M05, M06, M06HF, mPW1PW91, PBE, PBE0, TPSSh, VSXC, X3LYP) were used. The first frequency corresponding to phenyl moieties rotations was ignored when calculating the vibrational corrections $r_{h1} - r_a$.

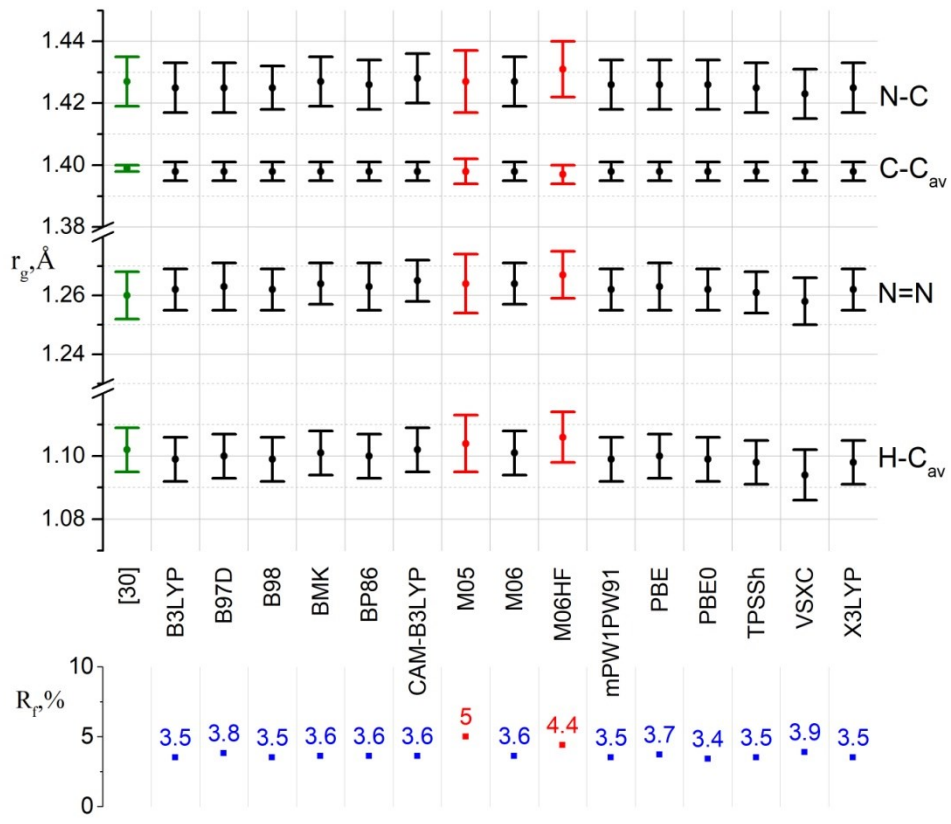


Figure S8. Results (r_g , R_f) of GED structural refinement for E-AB in the framework of MOCED method using starting parameters r_e , l , $r_{h1}-r_a$ obtained by different DFT calculations compared to results of S. Konaka and coworkers [30]. The results for LC-wPBE data were removed due to the completely unsatisfactory R_f value.

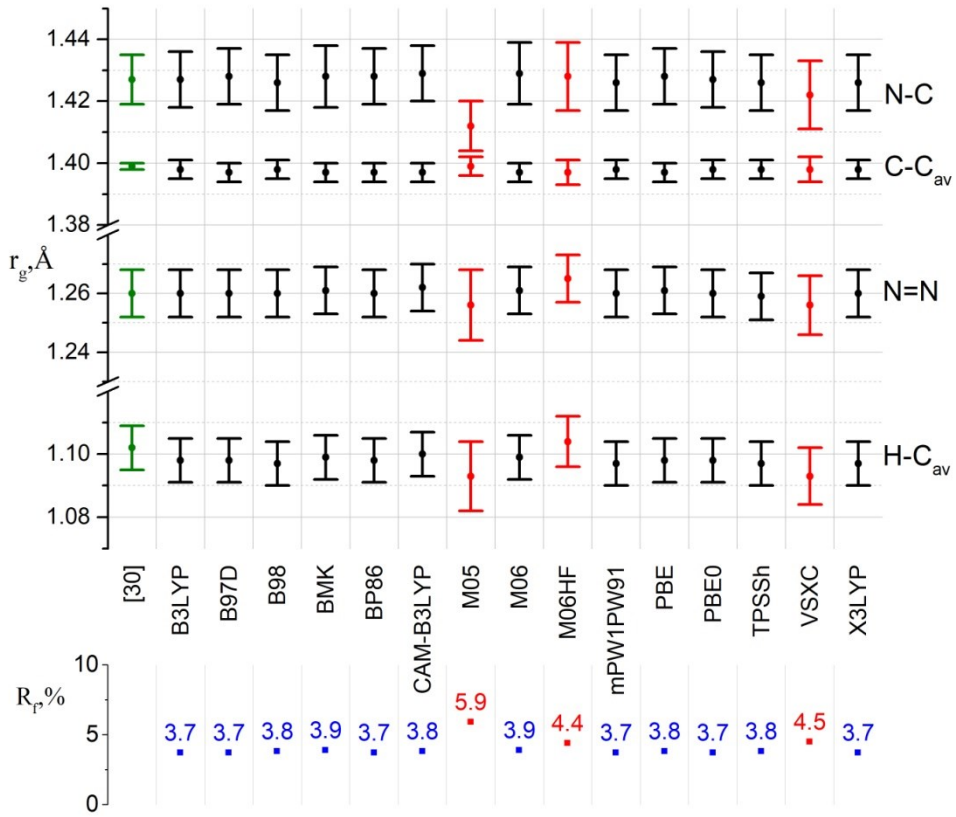


Figure S9. Results of GED structural refinement for E-AB in the framework of MOCED method using starting parameters r_e , l , r_e-r_a obtained by different DFT calculations compared to results of S. Konaka and coworkers [30]. The results for LC-wPBE data were removed due to the completely unsatisfactory R_f value.

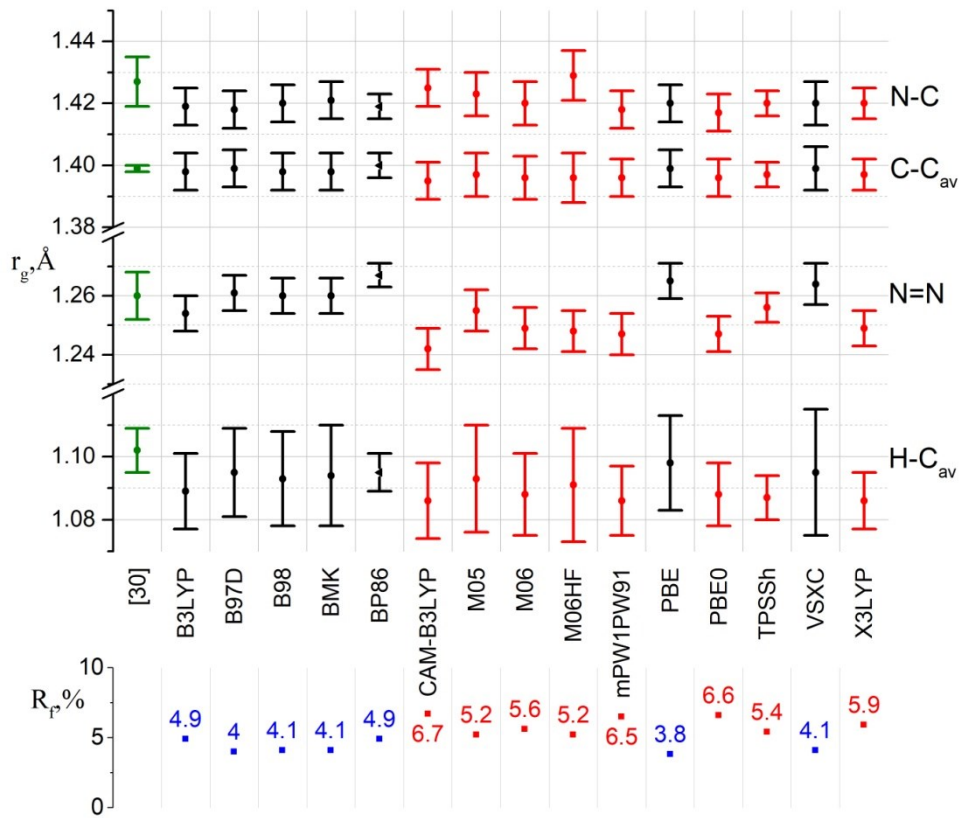


Figure S10. Results of GED structural refinement for E-AB in the framework of RM using starting parameters r_e , l , $r_{h1}-r_a$ obtained by different DFT calculations compared to results of S. Konaka and coworkers [30]. The results for LC-wPBE data were removed due to the completely unsatisfactory R_f value.

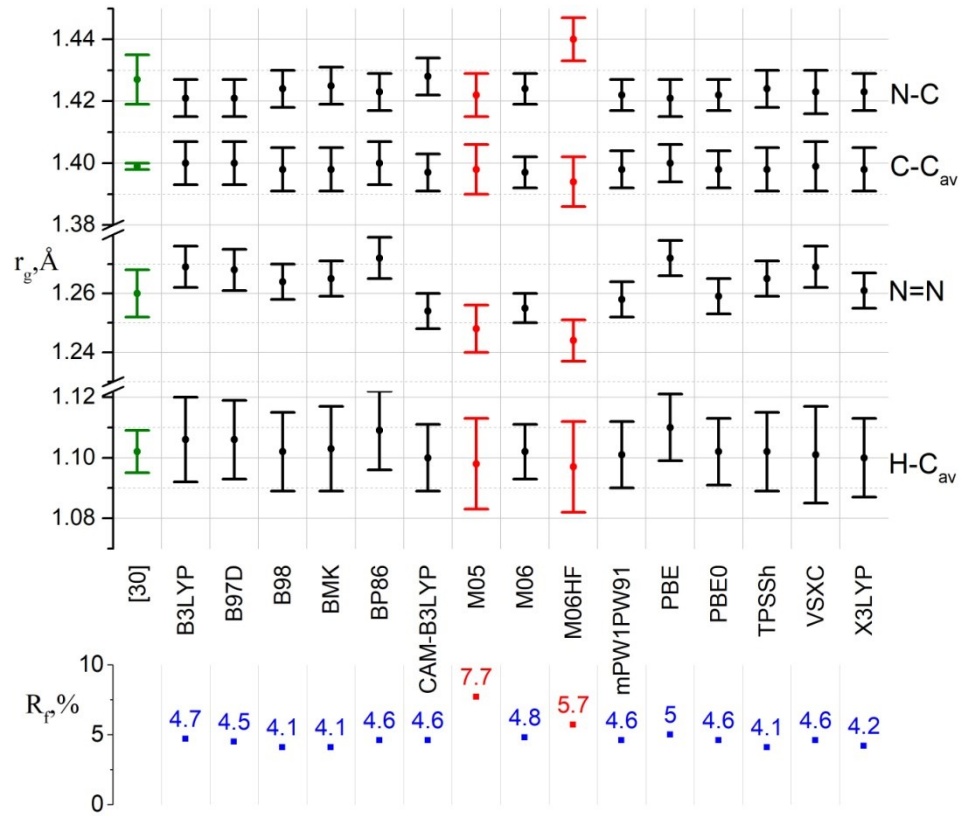


Figure S11. Results of GED structural refinement for E-AB in the framework of RM using starting parameters r_e , l , r_e-r_a obtained by different DFT calculations compared to results of S. Konaka and coworkers [30]. The results for LC-wPBE data were removed due to the completely unsatisfactory R_f value.

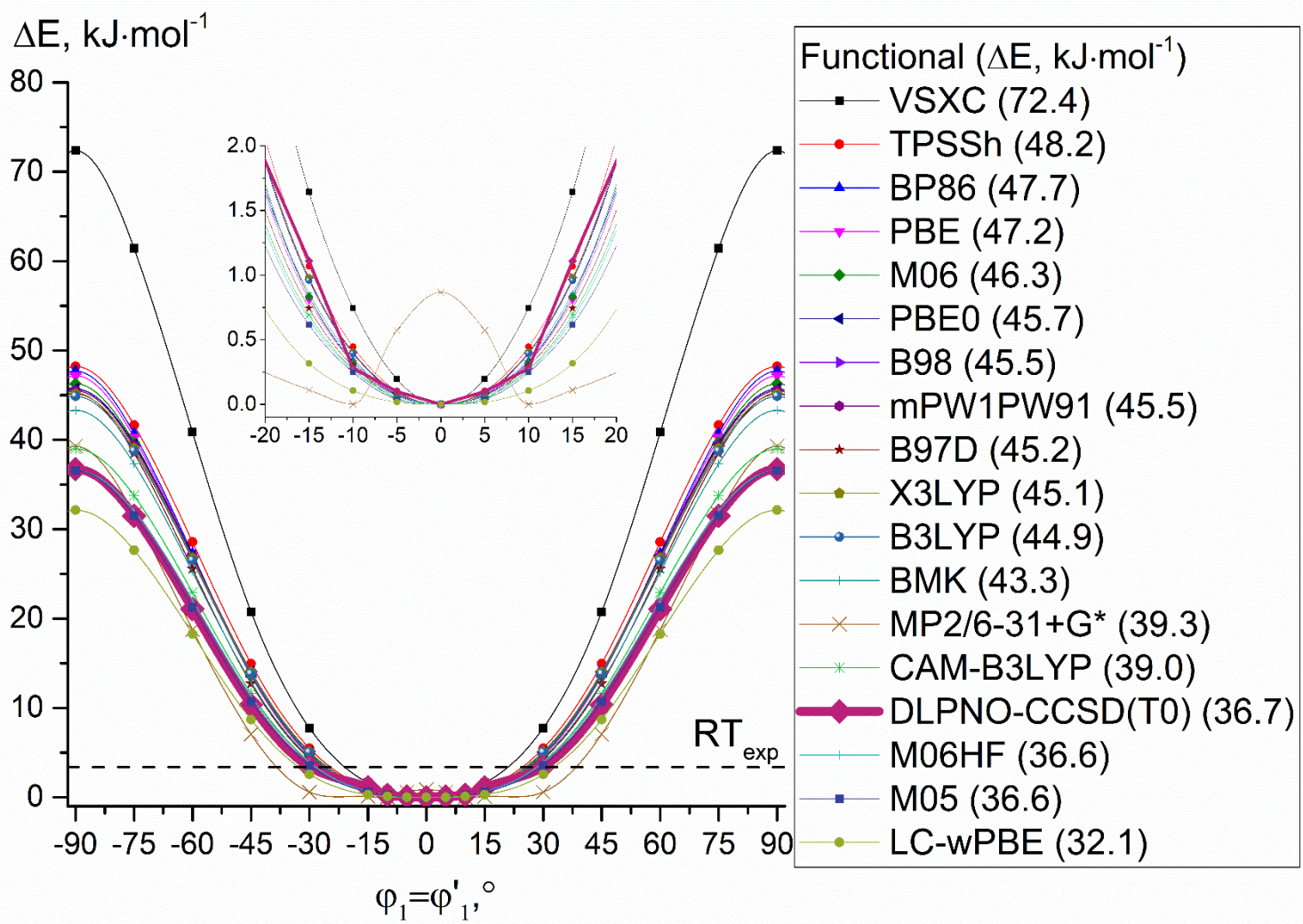


Figure S12. Potential energy function of simultaneous rotation of two phenyl rings around the $\text{N}_1\text{-C}_2$ and $\text{N}'_1\text{-C}'_2$ bonds in the E-AB molecule, calculated using different approximations. In all DFT calculations pcseg-2 basis set was used. DLPNO-CCSD(T0)/CBS was calculated using geometry optimized by B3LYP-D3/pcseg-2. Dashed line RT corresponds to the temperature of GED experiment ($T_{\text{exp}}=407$ K) [30].

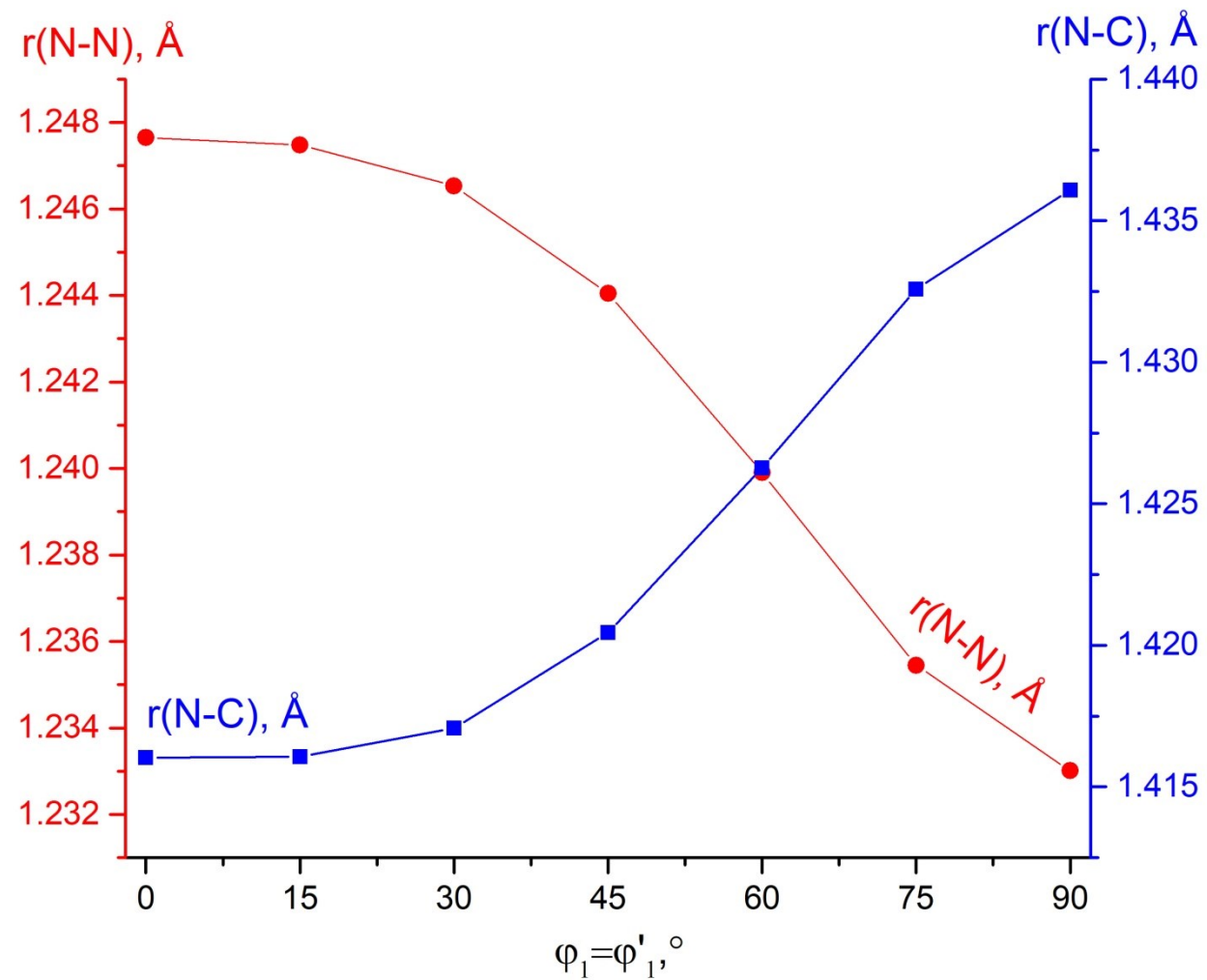


Figure S13. Internuclear distances $\text{N}_1\text{-N}'_1$ (red circles) and $\text{N}_1\text{-C}_2$ (blue squares) vs. dihedral angles φ_1 and φ'_1 in the E-AB molecule from the B3LYP-D3/pcseg-2 calculations.

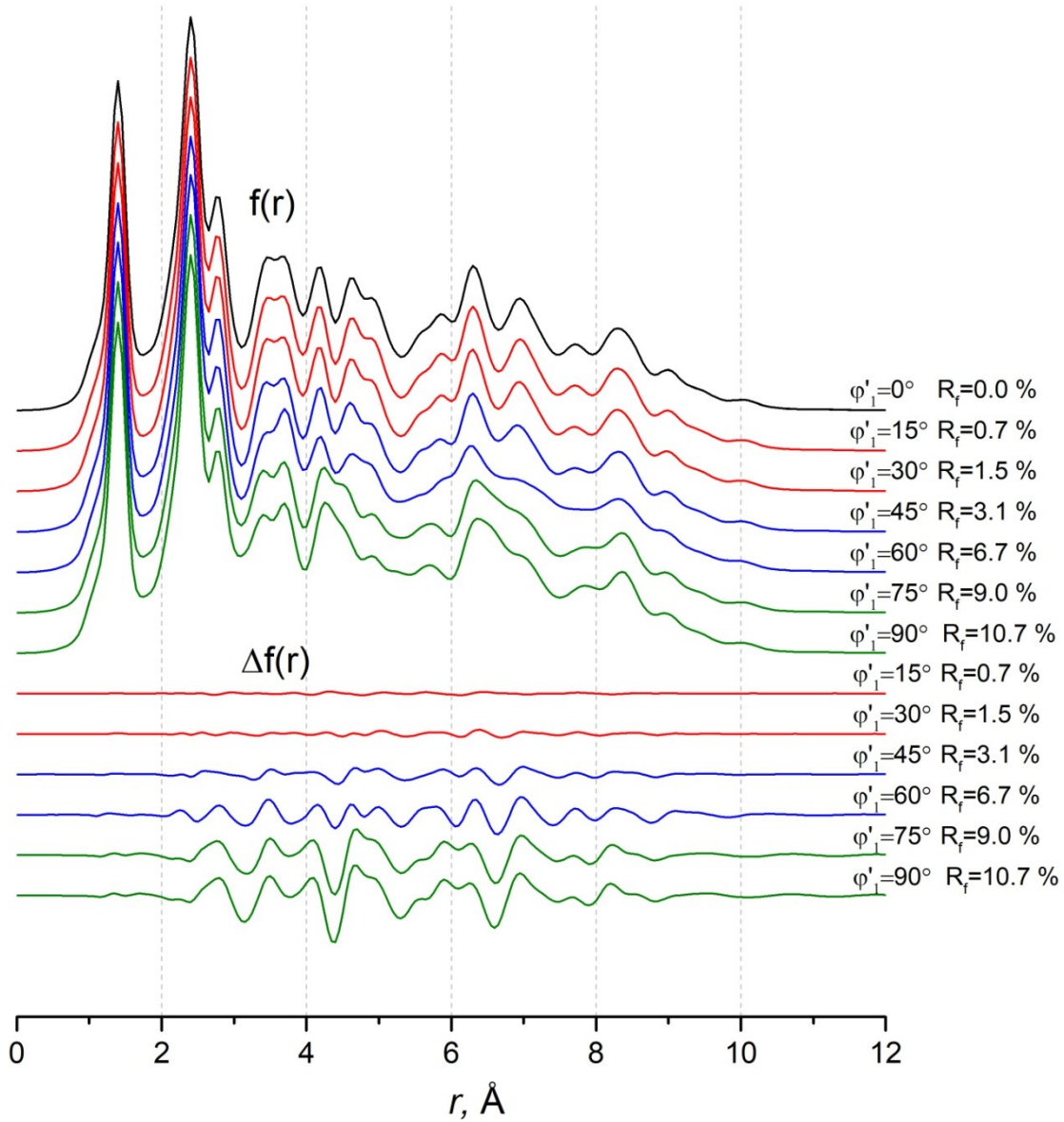


Figure S14. Comparison of theoretical radial distribution functions $f(r)$ of pseudoconformers of E-AB. Pseudoconformers obtained by rotation of one phenyl group were considered. Differences functions $\Delta f(r)$ were calculated concerning planar E-AB ($\varphi_1=\varphi'_1=0^\circ$). Molecular parameters were calculated at B3LYP-D3/pcseg-2 theory level. Vibrational amplitudes and corrections were obtained from the harmonic ($r_{\text{hi}}-r_a$) force fields using the VibModule program for the B3LYP-D3/pcseg-2 calculations (in cases of pseudoconformers with $\varphi'_1=60^\circ, 75^\circ, 90^\circ$, imaginary frequencies were considered as real).

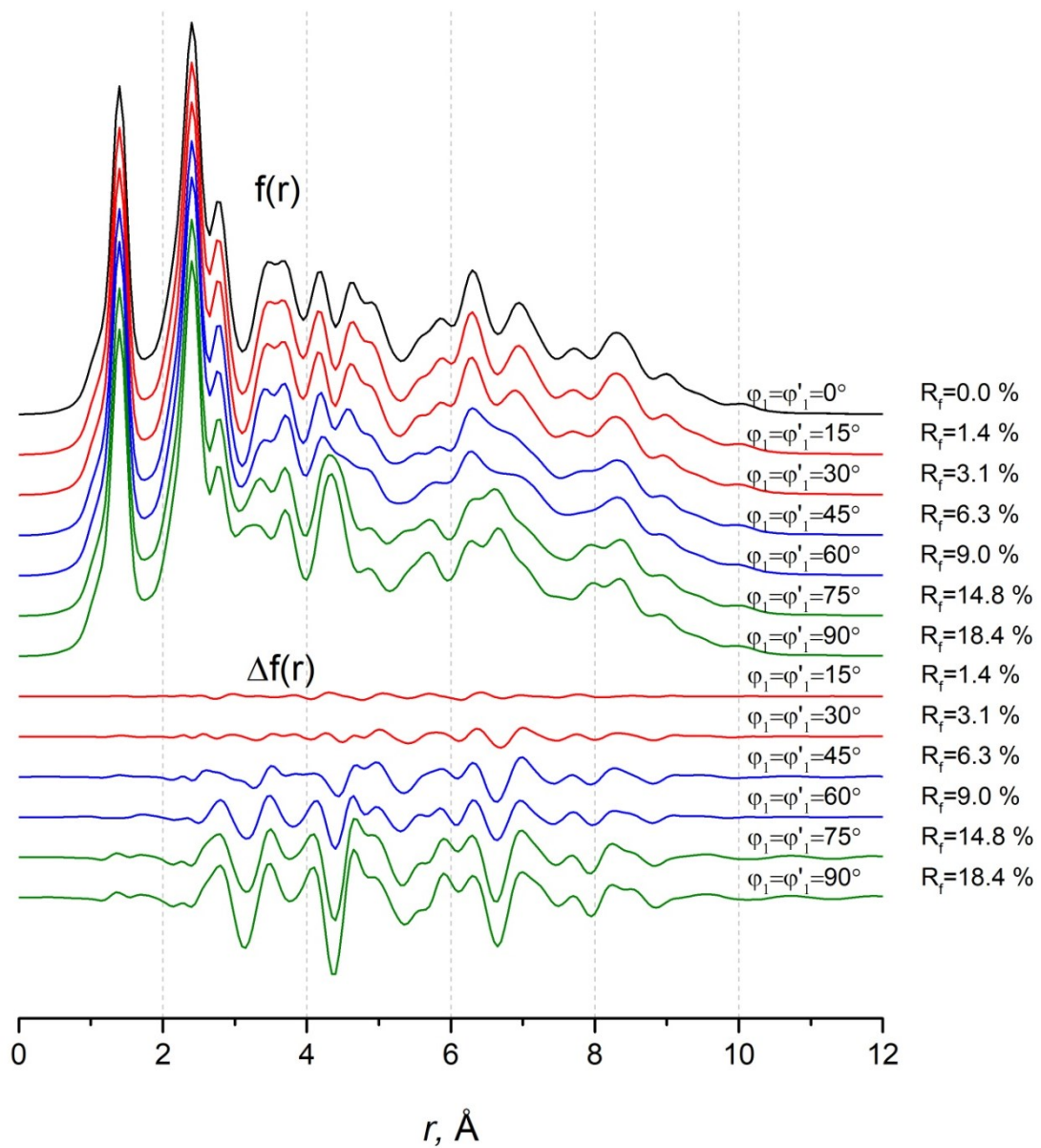


Figure S15. Comparison of theoretical radial distribution functions $f(r)$ of pseudoconformers of E-AB. Pseudoconformers obtained by rotation of two phenyl group were considered. Differences functions $\Delta f(r)$ were calculated concerning planar E-AB ($\varphi_1=\varphi'_1=0^\circ$). Molecular parameters were calculated at B3LYP-D3/pcseg-2 theory level. Vibrational amplitudes and corrections were obtained from the harmonic ($r_{h1}-r_a$) force fields using the VibModule program for the B3LYP-D3/pcseg-2 calculations (in cases of pseudoconformers with $\varphi_1=\varphi'_1=60^\circ, 75^\circ, 90^\circ$, imaginary frequencies were considered as real).

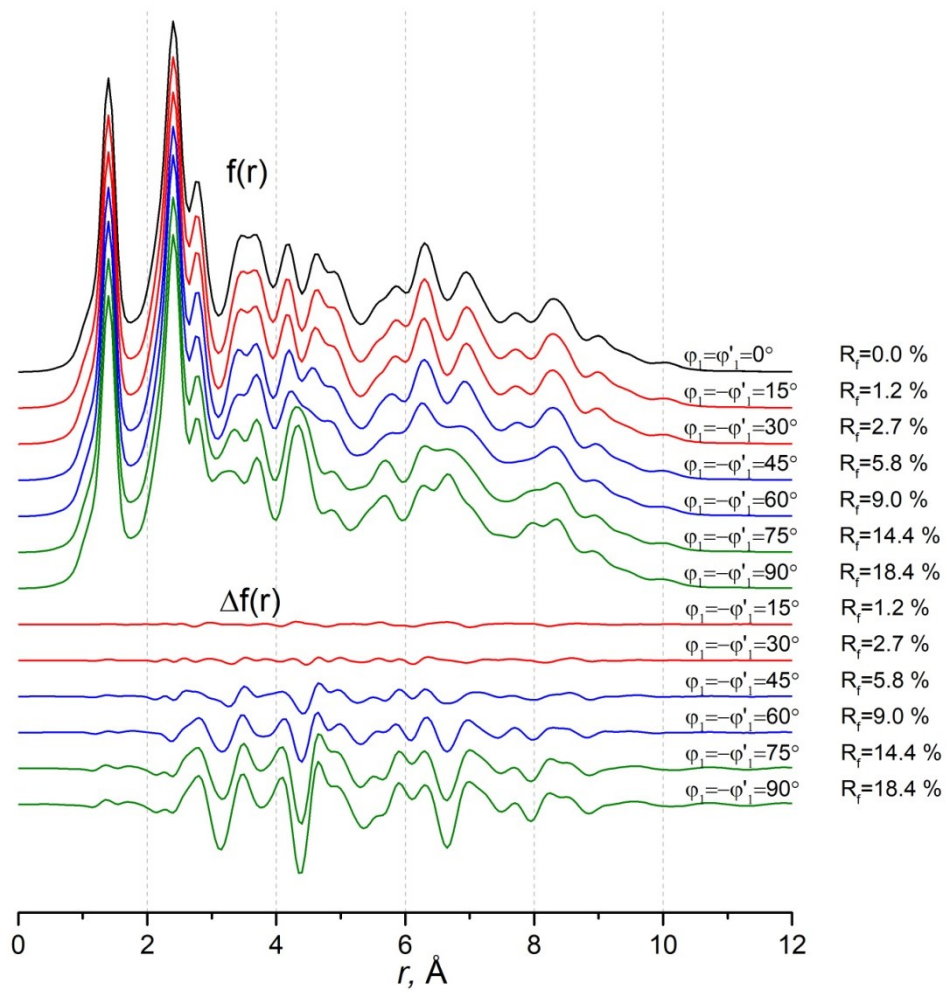


Figure S16. Comparison of theoretical radial distribution functions $f(r)$ of pseudoconformers of E-AB. Pseudoconformers obtained by rotation of two phenyl group were considered. Differences functions $\Delta f(r)$ were calculated concerning planar E-AB ($\varphi_1=\varphi'_1=0^\circ$). Molecular parameters were calculated at B3LYP-D3/pcseg-2 theory level. Vibrational amplitudes and corrections were obtained from the harmonic ($r_{h1}-r_a$) force fields using the VibModule program for the B3LYP-D3/pcseg-2 calculations (in cases of pseudoconformers with $\varphi_1=-\varphi'_1=60^\circ, 75^\circ, 90^\circ$, imaginary frequencies were considered as real).

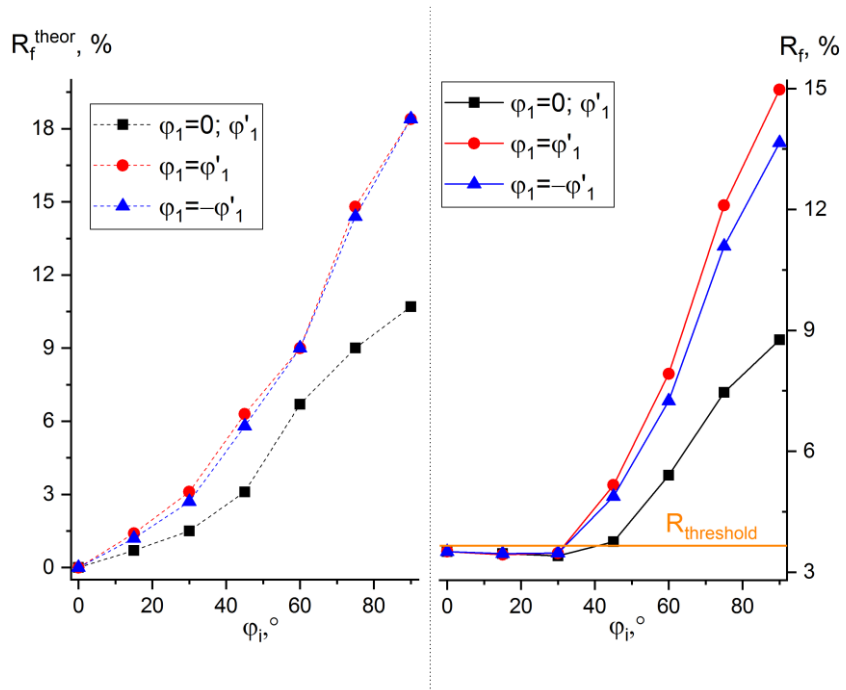


Table S1. Unex Z-matrix of E-AB

1	N							
2	N	1	NN					
3	C	1	RN1	2	AN1			
4	C	2	RN1_	1	AN1_	3	T	
5	C	3	RCC1	1	AC1	2	T1	
6	C	4	RCC1_	2	AC1_	1	T1_	
7	C	5	RCC2	3	AC2	1	T2	
8	C	6	RCC2_	4	AC2_	2	T2_	
9	C	7	RCC3	5	AC3	3	TPh1	
10	C	8	RCC3_	6	AC3_	4	TPh1_	
11	C	9	RCC4	7	AC4	5	TPh2	
12	C	10	RCC4_	8	AC4_	6	TPh2_	
13	C	3	RCC5	11	RCC6	5	TPh3	4
14	C	4	RCC5_	12	RCC6_	6	TPh3_	4
15	H	5	RCH1	3	ACH1	7	TH1	
16	H	6	RCH1_	4	ACH1_	8	TH1_	
17	H	7	RCH2	5	ACH2	9	TH2	
18	H	8	RCH2_	6	ACH2_	10	TH2_	
19	H	9	RCH3	7	ACH3	11	TH3	
20	H	10	RCH3_	8	ACH3_	12	TH3_	
21	H	11	RCH4	9	ACH4	13	TH4	
22	H	12	RCH4_	10	ACH4_	14	TH4_	
23	H	13	RCH5	3	ACH5	11	TH5	
24	H	14	RCH5_	4	ACH5_	12	TH5_	
1	N							
2	N	1	NN					
3	C	1	RN1	2	AN1			
4	C	2	RN1_	1	AN1_	3	T	
5	C	3	RCC1	1	AC1	2	T1	
6	C	4	RCC1_	2	AC1_	1	T1_	
7	C	5	RCC2	3	AC2	1	T2	
8	C	6	RCC2_	4	AC2_	2	T2_	
9	C	7	RCC3	5	AC3	3	TPh1	
10	C	8	RCC3_	6	AC3_	4	TPh1_	
11	C	9	RCC4	7	AC4	5	TPh2	
12	C	10	RCC4_	8	AC4_	6	TPh2_	

Table S2. Structural parameters (\AA) of E-AB according different DFT-calculations. A three-color-gradient scale indicates the ranking of parameters by values (green – maximal value of parameter, yellow – medium, red – minimal).

	B3LYP	B97D	B98	BMK	BP86	CAM-B3LYP	LC-wPBE	M05	M06	M06HF	mPW1 PW91	PBE0	PBE	TPSSh	VSXC	X3LYP	min	max	max – min	R ^a , %
$r_e(\text{N}_1=\text{N}'_1)$	1.248	1.260	1.250	1.250	1.267	1.235	1.229	1.243	1.242	1.221	1.242	1.242	1.265	1.255	1.260	1.246	1.221	1.267	0.045	3.6
$r_e(\text{N}_1-\text{C}_2)$	1.417	1.416	1.418	1.419	1.419	1.419	1.424	1.417	1.413	1.430	1.411	1.411	1.417	1.416	1.416	1.416	1.411	1.430	0.019	1.3
$r_e(\text{C}_2-\text{C}_3)$	1.400	1.410	1.402	1.401	1.409	1.392	1.387	1.396	1.393	1.392	1.395	1.396	1.408	1.401	1.405	1.399	1.387	1.410	0.023	1.6
$r_e(\text{C}_2-\text{C}_7)$	1.395	1.405	1.397	1.396	1.405	1.387	1.383	1.392	1.389	1.385	1.391	1.391	1.404	1.397	1.400	1.394	1.383	1.405	0.022	1.6
$r_e(\text{C}_3-\text{C}_4)$	1.384	1.391	1.386	1.387	1.391	1.380	1.378	1.382	1.379	1.383	1.381	1.381	1.390	1.385	1.389	1.384	1.378	1.391	0.013	1.0
$r_e(\text{C}_6-\text{C}_7)$	1.389	1.395	1.391	1.392	1.395	1.384	1.382	1.386	1.383	1.388	1.385	1.386	1.394	1.390	1.393	1.388	1.382	1.395	0.013	1.0
$r_e(\text{C}_4-\text{C}_5)$	1.395	1.403	1.397	1.398	1.404	1.389	1.386	1.392	1.389	1.392	1.391	1.392	1.402	1.397	1.402	1.395	1.386	1.404	0.017	1.2
$r_e(\text{C}_5-\text{C}_6)$	1.390	1.398	1.392	1.392	1.398	1.384	1.381	1.387	1.384	1.386	1.386	1.387	1.397	1.391	1.396	1.389	1.381	1.398	0.017	1.2
$r_e(\text{C}-\text{C})_{\text{av}}$	1.392	1.400	1.394	1.394	1.400	1.386	1.383	1.389	1.386	1.388	1.388	1.389	1.399	1.394	1.397	1.391	1.383	1.400	0.017	1.2
$\Delta r_e(\text{C}_i-\text{C}_j) = r_e(\text{C}_i-\text{C}_j) - r_e(\text{C}_2-\text{C}_3)$																				
$\Delta r_e(\text{C}_2-\text{C}_7)$	-0.005	-0.005	-0.005	-0.005	-0.004	-0.005	-0.005	-0.004	-0.004	-0.006	-0.005	-0.005	-0.004	-0.004	-0.005	-0.005	-0.006	-0.004	0.002	0.2
$\Delta r_e(\text{C}_3-\text{C}_4)$	-0.016	-0.020	-0.016	-0.014	-0.018	-0.012	-0.009	-0.015	-0.014	-0.009	-0.015	-0.015	-0.018	-0.016	-0.016	-0.015	-0.020	-0.009	0.011	0.8
$\Delta r_e(\text{C}_6-\text{C}_7)$	-0.011	-0.015	-0.011	-0.009	-0.014	-0.008	-0.005	-0.011	-0.010	-0.003	-0.011	-0.010	-0.014	-0.012	-0.012	-0.011	-0.015	-0.003	0.012	0.8
$\Delta r_e(\text{C}_4-\text{C}_5)$	-0.005	-0.007	-0.005	-0.003	-0.006	-0.003	-0.001	-0.004	-0.004	0.001	-0.004	-0.004	-0.006	-0.004	-0.003	-0.005	-0.007	0.001	0.008	0.6
$\Delta r_e(\text{C}_5-\text{C}_6)$	-0.010	-0.013	-0.010	-0.009	-0.011	-0.008	-0.006	-0.009	-0.009	-0.005	-0.009	-0.009	-0.011	-0.010	-0.009	-0.010	-0.013	-0.005	0.007	0.5
$\Delta r_e(\text{C}_i-\text{C}_j) = r_e(\text{C}_i-\text{C}_j) - r_e(\text{N}_1-\text{C}_2)$																				
$\Delta r_e(\text{C}_2-\text{C}_3)$	-0.017	-0.006	-0.016	-0.018	-0.010	-0.028	-0.037	-0.020	-0.019	-0.038	-0.016	-0.015	-0.009	-0.015	-0.011	-0.017	-0.038	-0.006	0.032	2.3
$\Delta r_e(\text{C}_2-\text{C}_7)$	-0.021	-0.011	-0.021	-0.023	-0.014	-0.033	-0.041	-0.024	-0.024	-0.044	-0.020	-0.020	-0.013	-0.020	-0.016	-0.022	-0.044	-0.011	0.033	2.4
$\Delta r_e(\text{C}_3-\text{C}_4)$	-0.032	-0.026	-0.032	-0.032	-0.028	-0.040	-0.046	-0.035	-0.034	-0.047	-0.030	-0.030	-0.027	-0.031	-0.027	-0.032	-0.047	-0.026	0.021	1.5
$\Delta r_e(\text{C}_6-\text{C}_7)$	-0.028	-0.021	-0.027	-0.027	-0.023	-0.035	-0.042	-0.031	-0.030	-0.042	-0.026	-0.025	-0.023	-0.027	-0.023	-0.028	-0.042	-0.021	0.021	1.5
$\Delta r_e(\text{C}_4-\text{C}_5)$	-0.022	-0.013	-0.021	-0.021	-0.015	-0.030	-0.038	-0.025	-0.023	-0.037	-0.020	-0.019	-0.015	-0.020	-0.014	-0.021	-0.038	-0.013	0.025	1.8
$\Delta r_e(\text{C}_5-\text{C}_6)$	-0.027	-0.019	-0.026	-0.027	-0.021	-0.036	-0.043	-0.030	-0.029	-0.044	-0.025	-0.024	-0.020	-0.025	-0.020	-0.027	-0.044	-0.019	0.025	1.8
$\Delta r_e(\text{X}_i-\text{X}_j) = r_e(\text{X}_i-\text{X}_j) - r_e(\text{N}_1=\text{N}'_1)$																				
$\Delta r_e(\text{N}_1-\text{C}_2)$	0.169	0.156	0.168	0.169	0.152	0.184	0.195	0.174	0.171	0.209	0.169	0.169	0.152	0.161	0.156	0.170	0.152	0.209	0.056	4.0
$\Delta r_e(\text{C}_2-\text{C}_3)$	0.152	0.150	0.152	0.151	0.143	0.157	0.158	0.154	0.152	0.170	0.154	0.154	0.143	0.146	0.144	0.153	0.143	0.170	0.028	2.0
$\Delta r_e(\text{C}_2-\text{C}_7)$	0.147	0.145	0.147	0.146	0.139	0.152	0.154	0.150	0.147	0.164	0.149	0.149	0.139	0.142	0.140	0.148	0.139	0.164	0.026	1.8
$\Delta r_e(\text{C}_3-\text{C}_4)$	0.136	0.131	0.136	0.137	0.125	0.145	0.149	0.139	0.137	0.162	0.139	0.139	0.126	0.130	0.129	0.137	0.125	0.162	0.037	2.7
$\Delta r_e(\text{C}_6-\text{C}_7)$	0.141	0.135	0.141	0.142	0.129	0.149	0.153	0.143	0.141	0.167	0.143	0.143	0.130	0.135	0.132	0.142	0.129	0.167	0.038	2.7
$\Delta r_e(\text{C}_4-\text{C}_5)$	0.147	0.143	0.147	0.148	0.137	0.154	0.157	0.149	0.148	0.171	0.150	0.150	0.138	0.142	0.142	0.148	0.137	0.171	0.034	2.5
$\Delta r_e(\text{C}_5-\text{C}_6)$	0.142	0.138	0.142	0.142	0.132	0.149	0.152	0.144	0.142	0.165	0.144	0.144	0.132	0.136	0.136	0.143	0.132	0.165	0.033	2.4

^a determined by equation (7).

Table S3. Relative energies ^{a,b} (ΔE , kJ·mol⁻¹) of E-AB according DLPNO-CCSD(T0) calculations. A three-color-gradient scale indicates the ranking of parameters by values (green – minimal value of ΔE , yellow – medium, red – maximal).

E-AB	B3LYP	B97D	B98	BMK	BP86	CAM-B3LYP	LC-wPBE	M05	M06	M06HF	mPW1PW91	PBE0	PBE	TPSSh	VSXC	X3LYP
DLPNO-CCSD(T0)/CBS ^c	0.5	2.8	0.2	0.0	3.7	2.4	4.0	0.9	2.2	3.1	1.5	1.4	3.1	0.1	0.9	0.6
DLPNO-CCSD(T0)/cc-pVQZ	0.7	2.1	0.2	0.0	2.8	3.2	5.0	1.4	3.0	4.0	2.2	2.0	2.3	0.1	0.5	0.9
DLPNO-CCSD(T0)/cc-pVTZ	1.4	1.1	0.4	0.2	1.5	4.9	7.1	2.5	4.6	5.7	3.6	3.2	1.3	0.4	0.0	1.7

^a $\Delta E_i^{E-Ab} = (E_i^{E-Ab} - E_{min}^{E-Ab}) \times 2625.5$, where i corresponds to the optimized geometry obtained by calculations using one of the considered DFT functionals.

^b DLPNO-CCSD(T0) calculations were performed using corresponding optimized geometries from DFT/pcseg-2 calculations.

Table S4. Relative energies ^{a,b} (ΔE , kJ·mol⁻¹) of Z-AB according DLPNO-CCSD(T0) calculations. A three-color-gradient scale indicates the ranking of parameters by values (green – minimal value of ΔE , yellow – medium, red – maximal).

	B3LYP	B97D	B98	BMK	BP86	CAM-B3LYP	LC-wPBE	M05	M06	M06HF	mPW1PW91	PBE0	PBE	TPSSh	VSXC	X3LYP
DLPNO-CCSD(T0)/CBS ^c	1.6	2.2	0.7	0.0	4.8	2.4	3.3	2.0	2.2	1.7	2.0	1.6	3.9	0.8	1.8	1.4
DLPNO-CCSD(T0)/cc-pVQZ	1.8	1.6	0.7	0.0	3.9	3.2	4.5	2.6	3.1	2.6	2.7	2.2	3.2	0.7	1.6	1.8
DLPNO-CCSD(T0)/cc-pVTZ	2.0	0.5	0.8	0.0	2.5	4.7	6.5	3.6	4.6	4.0	3.9	3.4	2.0	0.7	1.1	2.4

^a $\Delta E_i^{Z-Ab} = (E_i^{Z-Ab} - E_{min}^{Z-Ab}) \times 2625.5$, where i corresponds to the optimized geometry obtained by calculations using one of the considered DFT functionals.

^b DLPNO-CCSD(T0) calculations were performed using corresponding optimized geometries from DFT/pcseg-2 calculations.

Table S5. Energies ^{a,b} (ΔE , kJ·mol⁻¹) of Z-AB relative to the E-AB according DLPNO-CCSD(T0) calculations.

	B3LYP	B97D	B98	BMK	BP86	CAM-B3LYP	LC-wPBE	M05	M06	M06HF	mPW1PW91	PBE0	PBE	TPSSh	VSXC	X3LYP	ΔE_{min}	ΔE_{max}	$\Delta E_{max} - \Delta E_{min}$
DFT	63.2	44.0	61.2	60.0	57.6	62.0	55.5	54.5	55.2	52.4	61.0	60.2	56.2	59.6	42.7	63.4	42.7	63.4	20.6
DLPNO-CCSD(T0)/CBS ^c	51.8	50.0	51.2	50.7	51.7	50.7	50.0	51.8	50.7	49.3	51.2	50.9	51.5	51.4	51.6	51.5	49.3	51.8	2.5
DLPNO-CCSD(T0)/cc-pVQZ	51.9	50.3	51.4	50.9	52.0	50.9	50.3	52.0	51.0	49.5	51.4	51.2	51.8	51.5	52.0	51.7	49.5	52.0	2.6
DLPNO-CCSD(T0)/cc-pVTZ	52.1	50.9	51.8	51.2	52.4	51.3	50.9	52.5	51.5	49.7	51.8	51.7	52.2	51.8	52.6	52.2	49.7	52.6	2.9

^a $\Delta E_i = (E_i^{Z-Ab} - E_i^{E-Ab}) \times 2625.5$, where i corresponds to the optimized geometries obtained by calculations using one of the considered DFT functionals.

^b DLPNO-CCSD(T0) calculations were performed using corresponding optimized geometries from DFT/pcseg-2 calculations.

Table S6. Relative energies of pseudoconformers of E-AB and vibrational frequency of phenyls rotations according DFT^a, MP2 and DLPNO-CCSD(T0) calculations. A three-color-gradient scale indicates the ranking of parameters by values (green – maximal value of parameter, yellow – medium, red – minimal).

	B3LYP	B97D	B98	BMK	BP86	CAM-B3LYP	LC-wPBE	M05	M06	M06HF	mPW1PW91	PBE0	PBE	TPSSh	VSXC	X3LYP	DLPNO-CCSD(T0)/CBS ^b	DLPNO-CCSD(T0)/cc-pVQZ ^b	DLPNO-CCSD(T0)/cc-pVTZ ^b	MP2/6-31+G*
ΔE^c , kJ·mol ⁻¹ (conf-30)	5.0	4.3	5.1	4.5	4.8	4.0	2.6	3.6	4.9	3.9	5.1	5.1	4.7	5.5	7.8	5.1	3.4	3.6	3.8	-0.3
ΔE^d , kJ·mol ⁻¹ (conf-90)	44.9	45.2	45.5	43.3	47.7	39.0	32.1	36.6	46.3	36.6	45.5	45.7	47.2	48.2	72.4	45.1	36.7	37.2	38.0	39.3
$\omega_{\text{rot,Ph}}$, cm ⁻¹	19.4	17.3	19.1	17.1	17.4	16.1	6.6	11.4	16.2	12.3	19.8	19.3	16.6	20.3	28.6	19.8	-	-	-	11.5(i)

^a using pcseg-2 basis set;

^b using geometry optimized by B3LYP-D3/pcseg-2.

^c $\Delta E = E(\text{E-AB with } \varphi_1=\varphi'_1=30^\circ) - E(\text{E-AB with } \varphi_1=\varphi'_1=0^\circ)$;

^d $\Delta E = E(\text{E-AB with } \varphi_1=\varphi'_1=90^\circ) - E(\text{E-AB with } \varphi_1=\varphi'_1=0^\circ)$.

Table S7. Internuclear distances r_g of E-AB determined by MOCED structural analyzes using starting internuclear distances r_e , vibrational amplitudes l and corrections $r_e - r_a$ from results of different DFT calculations.

	[30] ^a	current work ^b															
Method ^c	MP2/ 6-31+G*	B3LYP	B97D	B98	BMK	BP86	CAM- B3LYP	LC-wPBE	M05	M06	M06HF	mPW1PW91	PBE	PBE0	TPSSh	VSXC	X3LYP
R_f^d		3.7	3.7	3.8	3.9	3.7	3.8	21.1	5.9	3.9	4.4	3.7	3.8	3.7	3.8	4.5	3.7
r_g (N-N)	1.260(8)	1.260(8)	1.260(8)	1.260(8)	1.261(8)	1.260(8)	1.262(8)	1.282(36)	1.256(12)	1.261(8)	1.265(8)	1.260(8)	1.261(8)	1.260(8)	1.259(8)	1.256(10)	1.260(8)
r_g (N-C)	1.427(8)	1.427(9)	1.428(9)	1.426(9)	1.428(10)	1.428(9)	1.429(9)	1.350(16)	1.412(8)	1.429(10)	1.428(11)	1.426(9)	1.428(9)	1.427(9)	1.426(9)	1.422(11)	1.426(9)
r_g (C-C) _{av}	1.399(1)	1.398(3)	1.397(3)	1.398(3)	1.397(3)	1.397(3)	1.397(3)	1.409(6)	1.399(3)	1.397(3)	1.397(4)	1.398(3)	1.397(3)	1.398(3)	1.398(3)	1.398(4)	1.398(3)
r_g (C-H) _{av}	1.102(7)	1.098(7)	1.098(7)	1.097(7)	1.099(7)	1.098(7)	1.100(7)	1.148(33)	1.093(11)	1.099(7)	1.104(8)	1.097(7)	1.098(7)	1.098(7)	1.097(7)	1.093(9)	1.097(7)
$R_f(0)^e$		8.5	18.8	11.0	12.7	18.7	8.7	32.6	12.0	8.1	15.0	7.6	16.4	7.5	9.0	13.4	7.8

^a uncertainties for the bond lengths were estimated as $3\sigma_{LS}$;

^b experimental data from ref. [30]; uncertainties for the bond lengths were estimated as $[(2.5\sigma_{LS})^2 + (0.002r)^2]^{1/2}$;

^c calculation method (DFT functional) that was used to obtain a set of initial parameters r_e , l and $r_e - r_a$; psceg-2 basis set was used in case of all DFT calculations;

^d disagreement factors R_f obtained in LS analyzes; a three-color-gradient scale indicates the ranking of parameters by values (green – minimal value of parameter, yellow – medium, red – maximal);

^e disagreement factor R_f obtained in first iteration of LS analyzes with refinement of scale factors for GED molecular intensity functions and without refinement of any structural parameters and vibrational amplitudes.

Table S8. Internuclear distances r_g of E-AB determined by MOCED structural analyzes using starting internuclear distances r_e , vibrational amplitudes l and corrections $r_{h1}-r_a$ from results of different DFT calculations.

	[30] ^a	current work ^b															
Method ^c	MP2/ 6-31+G*	B3LYP	B97D	B98	BMK	BP86	CAM- B3LYP	LC-wPBE	M05	M06	M06HF	mPW1PW91	PBE	PBE0	TPSSh	VSXC	X3LYP
R_f^d		3.5	3.8	3.5	3.6	3.6	3.6	17.9	5.0	3.6	4.4	3.5	3.7	3.4	3.5	3.9	3.5
$r_g(\text{N-N})$	1.260(8)	1.262(7)	1.263(8)	1.262(7)	1.264(7)	1.263(8)	1.265(7)	1.485(32)	1.264(10)	1.264(7)	1.267(8)	1.262(7)	1.263(8)	1.262(7)	1.261(7)	1.258(8)	1.262(7)
$r_g(\text{N-C})$	1.427(8)	1.425(8)	1.425(8)	1.425(7)	1.427(8)	1.426(8)	1.428(8)	1.264(18)	1.427(10)	1.427(8)	1.431(9)	1.426(8)	1.426(8)	1.426(8)	1.425(8)	1.423(8)	1.425(8)
$r_g(\text{C-C})_{\text{av}}$	1.399(1)	1.398(3)	1.398(3)	1.398(3)	1.398(3)	1.398(3)	1.398(3)	1.397(5)	1.398(4)	1.398(3)	1.397(3)	1.398(3)	1.398(3)	1.398(3)	1.398(3)	1.398(3)	1.398(3)
$r_g(\text{C-H})_{\text{av}}$	1.102(7)	1.099(7)	1.100(7)	1.099(7)	1.101(7)	1.100(7)	1.102(7)	1.086(26)	1.104(9)	1.101(7)	1.106(8)	1.099(7)	1.100(7)	1.099(7)	1.098(7)	1.094(8)	1.098(7)
$R_f(0)^e$		10.0	7.4	7.5	7.7	7.0	18.2	34.8	13.1	18.8	13.6	16.4	5.7	15.5	8.4	6.3	11.1

^a uncertainties for the bond lengths were estimated as $3\sigma_{LS}$;

^b experimental data from ref. [30]; uncertainties for the bond lengths were estimated as $[(2.5\sigma_{LS})^2 + (0.002r)^2]^{1/2}$;

^c calculation method (DFT functional) that was used to obtain a set of initial parameters r_e , l and $r_{h1}-r_a$; psceg-2 basis set was used in case of all DFT calculations;

^d disagreement factors R_f obtained in LS analyzes; a three-color-gradient scale indicates the ranking of parameters by values (green – minimal value of parameter, yellow – medium, red – maximal);

^e disagreement factor R_f obtained in first iteration of LS analyzes with refinement of scale factors for GED molecular intensity functions and without refinement of any structural parameters and vibrational amplitudes.

Table S9. Internuclear distances r_g and corresponding contribution of experimental GED data to parameters (w) of E-AB determined by RM structural analyzes using starting internuclear distances r_e , vibrational amplitudes l and corrections r_e-r_a from results of different DFT calculations.

	[30] ^a	current work ^b															
Method ^c	MP2/ 6-31+G*	B3LYP	B97D	B98	BMK	BP86	CAM-B3LYP	LC-wPBE	M05	M06	M06HF	mPW1PW91	PBE	PBE0	TPSSh	VSXC	X3LYP
α_{reg}^d		0.002	0.002	0.001 ^e	0.001 ^e	0.002	0.002	0.0005	0.003	0.004	0.002	0.002	0.004	0.002	0.001 ^e	0.001 ^e	0.001
R_f^f		4.7	4.5	4.1	4.1	4.6	4.6	12.4	7.7	4.8	5.7	4.6	5.0	4.6	4.1	4.6	4.2
r_g (N-N)	1.260(8)	1.269(7)	1.268(7)	1.264(6)	1.265(6)	1.272(7)	1.254(6)	1.238(18)	1.248(8)	1.255(5)	1.244(7)	1.258(6)	1.272(6)	1.259(6)	1.265(6)	1.269(7)	1.261(6)
r_g (C-N)	1.427(8)	1.421(6)	1.421(6)	1.424(6)	1.425(6)	1.423(6)	1.428(6)	1.407(24)	1.422(7)	1.424(5)	1.440(7)	1.422(5)	1.421(6)	1.422(5)	1.424(6)	1.423(7)	1.423(6)
r_g (C-C) _{av}	1.399(1)	1.400(7)	1.400(7)	1.398(7)	1.398(7)	1.400(7)	1.397(6)	1.397(28)	1.398(8)	1.397(5)	1.394(8)	1.398(6)	1.400(6)	1.398(6)	1.398(7)	1.399(8)	1.398(7)
r_g (H-C) _{av}	1.102(7)	1.106(14)	1.106(13)	1.102(13)	1.103(14)	1.109(13)	1.100(11)	1.100(59)	1.098(15)	1.102(9)	1.097(15)	1.101(11)	1.110(11)	1.102(11)	1.102(13)	1.101(16)	1.100(13)
w (N-N)	-	0.71	0.71	0.83	0.83	0.70	0.72	0.97	0.65	0.56	0.74	0.72	0.54	0.72	0.83	0.83	0.83
w (C-N)	-	0.69	0.69	0.82	0.82	0.69	0.70	0.97	0.61	0.54	0.71	0.70	0.53	0.70	0.81	0.82	0.82
w (C-C) _{av}	-	0.69	0.69	0.81	0.81	0.69	0.69	0.95	0.61	0.53	0.70	0.69	0.53	0.69	0.81	0.82	0.81
w (H-C) _{av}	-	0.10	0.10	0.17	0.17	0.10	0.10	0.57	0.07	0.05	0.10	0.09	0.05	0.09	0.18	0.17	0.17
$R_f(0)^g$	-	8.5	18.8	11.0	12.7	18.7	8.7	32.6	12.0	8.1	15.0	7.6	16.4	7.5	9.0	13.4	7.8

^a uncertainties for the bond lengths were estimated as $3\sigma_{LS}$;

^b experimental data from ref. [30]; uncertainties for the bond lengths were estimated as $[(2.5\sigma_{LS})^2 + (0.002r)^2]^{1/2}$;

^c calculation method (DFT functional) that was used to obtain a set of initial parameters r_e , l and r_e-r_a ; psceg-2 basis set was used in case of all DFT calculations;

^d regularization constant α_{reg} , which was chosen according to Eq. (3);

^e for these initial parameters, the minimum of α_{reg} in the range from $6 \cdot 10^{-5}$ to 0.01 was not found, therefore, a value of 0.001 was chosen;

^f disagreement factors R_f obtained in LS analyzes; a three-color-gradient scale indicates the ranking of parameters by values (green – minimal value of parameter, yellow – medium, red – maximal);

^g disagreement factor R_f obtained in first iteration of LS analyzes with refinement of scale factors for GED molecular intensity functions and without refinement of any structural parameters and vibrational amplitudes.

Table S10. Internuclear distances r_g and corresponding contribution of experimental GED data to parameters (w) of E-AB determined by RM structural analyzes using starting internuclear distances r_e , vibrational amplitudes l and corrections $r_{h1}-r_a$ from results of different DFT calculations in comparison with results of the work [30].

	[30] ^a	current work ^b															
Method ^c	MP2/6-31+G*	B3LYP	B97D	B98	BMK	BP86	CAM-B3LYP	LC-wPBE	M05	M06	M06HF	mPW1PW91	PBE	PBE0	TPSSh	VSXC	X3LYP
α_{reg}^d		0.002	0.0008	0.0007	0.0007	0.009	0.005	0.0009	0.001 ^e	0.003	0.001	0.006	0.0006	0.007	0.009	0.0004	0.006
R_f^f		4.9	4.0	4.1	4.1	4.9	6.7	12.6	5.2	5.6	5.2	6.5	3.8	6.6	5.4	4.1	5.9
$r_g(N-N)$	1.260(8)	1.254(6)	1.261(6)	1.260(6)	1.260(6)	1.267(4)	1.242(7)	1.250(17)	1.255(7)	1.249(7)	1.248(7)	1.247(7)	1.265(6)	1.247(6)	1.256(5)	1.264(7)	1.249(6)
$r_g(C-N)$	1.427(8)	1.419(6)	1.418(6)	1.420(6)	1.421(6)	1.419(4)	1.425(6)	1.464(17)	1.423(7)	1.420(7)	1.429(8)	1.418(6)	1.420(6)	1.417(6)	1.420(4)	1.420(7)	1.420(5)
$r_g(C-C)_{av}$	1.399(1)	1.398(6)	1.399(6)	1.398(6)	1.398(6)	1.400(4)	1.395(6)	1.392(17)	1.397(7)	1.396(7)	1.396(8)	1.396(6)	1.399(6)	1.396(6)	1.397(4)	1.399(7)	1.397(5)
$r_g(H-C)_{av}$	1.102(7)	1.089(12)	1.095(14)	1.093(15)	1.094(16)	1.095(6)	1.086(12)	1.087(51)	1.093(17)	1.088(13)	1.091(18)	1.086(11)	1.098(15)	1.088(10)	1.087(7)	1.095(20)	1.086(9)
$w(N-N)$	-	0.72	0.86	0.88	0.88	0.35	0.51	0.92	0.83	0.63	0.84	0.46	0.89	0.43	0.36	0.93	0.46
$w(C-N)$	-	0.69	0.84	0.86	0.86	0.34	0.48	0.91	0.81	0.60	0.82	0.44	0.88	0.41	0.34	0.92	0.44
$w(C-C)_{av}$	-	0.69	0.84	0.86	0.86	0.34	0.48	0.88	0.81	0.60	0.82	0.43	0.88	0.39	0.34	0.92	0.43
$w(H-C)_{av}$	-	0.10	0.21	0.23	0.23	0.02	0.04	0.30	0.18	0.07	0.18	0.03	0.26	0.03	0.02	0.34	0.04
$R_f(0)^g$	-	10.0	7.4	7.5	7.7	7.0	18.2	34.8	13.1	18.8	13.6	16.4	5.7	15.5	8.4	6.3	11.1

^a uncertainties for the bond lengths were estimated as $3\sigma_{LS}$;

^b experimental data from ref. [30]; uncertainties for the bond lengths were estimated as $[(2.5\sigma_{LS})^2 + (0.002r)^2]^{1/2}$;

^c calculation method (DFT functional) that was used to obtain a set of initial parameters r_e , l and $r_{h1}-r_a$; psceg-2 basis set was used in case of all DFT calculations;

^d regularization constant α_{reg} , which was chosen according to Eq. (3);

^e for these initial parameters, the minimum of α_{reg} in the range from $6 \cdot 10^{-5}$ to 0.01 was not found, therefore, a value of 0.001 was chosen;

^f disagreement factors R_f obtained in LS analyzes; a three-color-gradient scale indicates the ranking of parameters by values (green – minimal value of parameter, yellow – medium, red – maximal);

^g disagreement factors R_f obtained in first iteration of LS analyzes with refinement of scale factors for GED molecular intensity functions and without refinement of any structural parameters and vibrational amplitudes.

Table S11. Cartesian atomic coordinates of final semiexperimental equilibrium structure (r_e) of E-AB according GED method ($R=3.7\%$, experimental data – from ref. [30], structural refinement – from our work: MOCED, semirigid model, starting parameters from B3LYP-D3/pcseg-2 calculations).

	x	y	z
N	-0.3779954858	0.5006359865	0.0000000016
N	0.3779954858	-0.5006359865	0.0000000016
C	-1.7594962368	0.1859605794	0.0000000016
C	1.7594962368	-0.1859605794	0.0000000016
C	-2.2778763098	-1.1114912717	0.0000000015
C	2.2778763098	1.1114912717	0.0000000015
C	-3.6466799365	-1.2983477821	0.0000000015
C	3.6466799365	1.2983477821	0.0000000015
C	-4.5080908248	-0.2043816279	0.0000000016
C	4.5080908248	0.2043816279	0.0000000016
C	-3.9919335812	1.0828481558	0.0000000016
C	3.9919335812	-1.0828481558	0.0000000016
C	-2.6203600841	1.2805227620	-0.0000000087
C	2.6203600841	-1.2805227620	-0.0000000087
H	-1.6008485979	-1.9460830373	0.0000000014
H	1.6008485979	1.9460830373	0.0000000014
H	-4.0493892918	-2.2973129109	0.0000000015
H	4.0493892918	2.2973129109	0.0000000015
H	-5.5737527889	-0.3593080475	0.0000000016
H	5.5737527889	0.3593080475	0.0000000016
H	-4.6543744582	1.9315510369	0.0000000097
H	4.6543744582	-1.9315510369	0.0000000097
H	-2.1932171887	2.2684866754	-0.0000000247
H	2.1932171887	-2.2684866754	-0.0000000247

[30] Tsuji, T.; Takashima, H.; Takeuchi, H.; Egawa, T.; Konaka, S. Molecular Structure and Torsional Potential of trans-Azobenzene. A Gas Electron Diffraction Study. *J. Phys. Chem. A* 2001, 105, 9347–9353, doi:10.1021/jp004418v

[91] Hamilton, W.C. Significance tests on the crystallographic R factor. *Acta Crystallogr.* 1965, 18, 502–510, doi:10.1107/S0365110X65001081